Structural and optical properties of (100) InAs single-monolayer quantum wells in bulklike GaAs grown by molecular-beam epitaxy

O. Brandt, L. Tapfer, R. Cingolani, and K. Ploog
Max-Planck-Institut für Festkörperforschung, Postfach 80 06 65, D-7000 Stuttgart 80, Federal Republic of Germany

M. Hohenstein and F. Phillipp
Max-Planck-Institut für Metallforschung, Postfach 80 06 65, D-7000 Stuttgart 80, Federal Republic of Germany
(Received 29 January 1990)

A single (100) monolayer InAs in GaAs is grown by conventional molecular-beam epitaxy. The structural properties of these highly strained single-monolayer quantum-well samples are investigated with high-resolution double-crystal x-ray diffractometry, double-crystal x-ray reflection topography, and transmission electron microscopy. The calculation of the x-ray-diffraction patterns within the framework of the dynamical diffraction theory provides the precise determination of the strain state and the thickness of the layer even in the submonolayer region. This approach allows us to prove the superior crystalline quality of the samples. In particular, no misfit dislocations are generated at the highly strained InAs/GaAs heterointerface as observed by x-ray topography. These results are confirmed by the high-resolution lattice image of the heterointerface, indicating the excellent homogeneity and flatness of the InAs lattice plane. In addition, we present evidence for a strong impact of the strain on the incorporation of cations in the crystal lattice during epitaxial growth. This structural information on an atomic scale is necessary for a correct interpretation of photoluminescence (PL) and photoluminescence excitation (PLE) spectra. We correlate the results of our structural investigation with a simple analysis of the PL linewidth and the blue shift (Stokes shift) of the heavy-hole exciton resonance in the PLE spectrum with respect to the electron heavy-hole transition in the PL spectrum. Both the PL linewidth and the Stokes shift are explained in terms of a fluctuation of the well width of 1 monolayer and a lateral island size of about 10 nm, in excellent agreement with the lattice image of the structure. The important result of our investigation is that a single monolayer of InAs yields a pronounced redshift of the quantum-well luminescence as compared with that of bulklike GaAs. Additionally, the PLE spectrum provides direct experimental evidence for a weak confinement of the light-hole excitons in the InAs plane. This result clearly indicates a type-I band alignment for both heavy holes and light holes, as predicted by a simple envelope-function calculation. Finally, the samples exhibit a surprisingly high luminescence efficiency, resulting from a very efficient trapping of the photoexcited carriers into the InAs-monolayer quantum well with trapping times of the order of only 20 ps.

I. INTRODUCTION

Highly strained semiconductor systems are interesting from a fundamental point of view due to their unique electronic and optical properties as well as for potential applications in electronic and optoelectronic devices.[1] Among these systems, the (In,Ga)As/GaAs heterojunction is an ideal candidate to study the structural and optical properties of highly strained layers.[2,3] In addition, in the first stage of growth this material system provides a detailed insight into the fundamental growth modes of heteroepitaxy.[4] Recent advances in the epitaxial growth techniques[5–7] have allowed us to fabricate high-quality InAs/GaAs single–quantum-well structures with high luminescence efficiencies and narrow linewidths. However, despite its importance, up to now only little knowledge has been acquired about the actual structural properties of these ultrathin quantum wells. The growth of InAs on GaAs is known to be strongly influenced by the large lattice mismatch ($\epsilon = 7.16\%$) between GaAs and InAs.[2,4] For instance, in the monolayer region a lower growth rate is expected because of the lower In incorporation compared with the bulk case as found in desorption measurements.[8] In accordance with this observation, recently published investigations[9] of the metalorganic vapor-phase epitaxy (MOVPE) growth of highly strained $In_xGa_{1-x}As/GaAs$ ($0 \leq x \leq 1$) suggested a hindered In incorporation in the strained lattice. The growth of pure InAs was found to be even impossible, which the authors attributed to a compositional mixing at the strained interface, probably supported by the complex adsorption-desorption processes resulting from the MOVPE reaction kinetics. With increasing growth temperature, a considerable In desorption and migration can take place and can strongly influence the actual structural properties of the layers.[10,11] Since the physical properties depend critically on the actual amount of In and the thickness of the quantum well, a correct interpretation of the optical and electrical measurements is only possible with an exact knowledge of the structural properties of the strained layer.

This paper reports a detailed investigation of structural and optical properties of a monolayer of InAs inserted in bulklike GaAs, growth for the first time by conventional

solid-source molecular-beam epitaxy (MBE). The results are based on a comparative study of high-resolution double-crystal x-ray diffractometry (HRDXD), double-crystal x-ray reflection topography, high-resolution transmission electron microscopy (HRTEM), low-temperature photoluminescence (PL), and photoluminescence excitation (PLE) spectroscopy.

II. EXPERIMENT

The InAs/GaAs structures are grown in a three–vacuum-chamber MBE system, which is equipped with elemental solid sources and an azimuthally rotating substrate holder. The substrate rotation is synchronized to the shutter operation by using an integer number of rotations per growth time of each constituent layer.

The investigated samples consist of a 1-μm-thick GaAs buffer layer grown at 540 °C on semi-insulating (100) GaAs substrates, a monolayer InAs grown at 420 °C, and a 200-nm-thick GaAs cap layer grown again at 540 °C. To avoid In desorption completely a few monolayers of GaAs are deposited at 420 ° C on top on the InAs layer, before heating up again to 540 °C. The reference for the calibration of the substrate temperature is given by the desorption of the native oxide at 580 °C observed in the RHEED (reflection high-energy electron diffraction) pattern. The established As- to Ga-flux ratio of $j_{As_4}/j_{Ga}=1$ corresponds to an As-stabilized surface as indicated by the sharp (2×4) reconstruction during growth. The InAs plane is grown near the boundary to the In-rich region, as manifested by a sharp transition to a (4×1) reconstruction for a slightly increased growth temperature of 430 °C. However, although the quality of *bulk* InAs depends critically on the As- to In-flux ratio, we do not observe any difference in the structural and optical properties of samples grown under the conditions of $j_{As_4}/j_{In}=2$ and under strongly As-stabilized conditions ($j_{As_4}/j_{In}=7$), respectively. Indeed, the accumulation of excess As_4 on the growing surface is expected to be much less critical for 1 ML of InAs than for bulk InAs, where excess As is incorporated in the crystal. Instead we found it essential to maintain a rather low growth rate of about 0.2 Å/s during the deposition of InAs. Higher growth rates result in a dramatic deterioration of the optical properties of the layers, as will be described later. To obtain small fluctuations of the well width, the InAs layer is annealed for 120 s before we grow the cap layer. This procedure leads to a sharpening of the reconstruction streaks in the RHEED pattern, which could be interpreted as a smoothing of the growth surface.

The x-ray measurements are performed with a computer-controlled high-resolution double-crystal x-ray diffractometer, utilizing a rotating-anode 12-kW generator with a copper target ($\lambda_{Cu\ K\alpha_1}=1.540\,562$ Å). A well-defined monochromatic x-ray beam is obtained by using an asymmetrically cut, dislocation free (100) Ge crystal and the (400) reflection. Symmetric (400) as well as asymmetric (422) diffraction patterns are routinely recorded in the reflection mode (Bragg case).

The cross-sectional samples for the HRTEM investigation are prepared by the conventional sandwich technique, cut into ⟨110⟩ slices, thinned, dimpled, and ion milled. The specimen thickness in the investigated area is then approximately 20 nm. The pictures are taken in a JEOL 4000EX microscope. Diffracted beams up to the {400} reflection are included in the diffraction aperture.

PL and PLE measurements are carried out with the samples at 4.2 K using the red line (647.6 nm) of a Kr^+ laser or a conventional 150-W halogen lamp as an excitation source, respectively. The light of the halogen lamp is dispersed by a 0.6-m double-grating monochromator in the infrared range. The emitted luminescence light is dispersed by a 1-m single-grating monochromator and detected either with a liquid-nitrogen-cooled Ge detector and standard lock-in amplification or by photon counting techniques with the use of a photomultiplier. A wide range of excitation densities is used. The PL spectra are taken with excitation densities up to 100 W/cm^2. The PLE measurements are performed at 10^{-4}W/cm^2.

III. RESULTS

A. Structural properties

It has been shown recently that the interference of x-ray wave fields in semiconductor heterostructures can be used to analyze ultrathin layers in the nm range.[12] This technique has been applied to detect individual Ge layers in Si having a thickness of only one monolayer (1 ML).[13] The HRDXD technique thus allows us to determine the structural properties of ultrathin layers with high precision, in particular the lattice strain and the layer thickness. However, a computer simulation of the experimental diffraction pattern is required in order to obtain this detailed structural information.

The incident x-ray wave field is scattered by the GaAs substrate and the GaAs cap layer simultaneously, i.e., at identical Bragg angle. However, the wave diffracted from the GaAs cap layer is *decoupled* and *phase shifted* with respect to the wave scattered from the GaAs substrate. The phase shift is caused by the different lattice constant of the sandwiched InAs plane and is enhanced by the tetragonal distortion of the unit cell. Provided that no strain relaxation occurs, the distance between the In and As atoms can be determined to be 1.6246 Å in the ⟨100⟩ direction. The interference between the two wave fields scattered by the GaAs cap layer and the GaAs substrate can be observed in the x-ray-diffraction pattern as the *Pendellösung* effect. This interference effect is strongly influenced by the lattice strain and thickness of the sandwiched InAs layer. Thus, the *Pendellösung* fringes are modulated by the decoupling and phase shifting of the scattered wave fields. However, the angular distance ω between the interference fringes is still given by the thickness Δ of the GaAs cap layer:

$$\omega=\frac{\lambda|\gamma_h|}{\Delta\sin(2\Theta_B)}\ , \tag{1}$$

where λ is the x-ray wavelength ($\lambda_{Cu\ K\alpha_1}=1.540\,562$ Å), Θ_B is the kinematic Bragg angle, and $\gamma_h=\cos[\pi/2$

TABLE I. Parameters used for the simulation of the x-ray-diffraction patterns and for the calculation of the subband energies. All values are taken from Ref. 16 unless otherwise noted.

Parameter	GaAs	InAs
Lattice constant a_0 (Å)	5.653 25	6.0583
Elastic stiffness constants (10^{10} Pa)		
C_{11}	11.88	8.329
C_{22}	5.38	4.526
C_{44}	5.95	3.959
Structure factors[a]		
F_r (400)	153.74	205.85
F_i (400)	7.13	24.20
F_r (422)	134.82	182.65
F_i (422)	7.13	24.20
F_r (000)	246.54	323.45
F_i (000)	7.13	24.20
Pressure dependence of the direct gap		
dE_Γ/dP (10^{-11} eV/Pa)	10.7	10.2
Shear deformation potential b (eV)	−1.7	−1.8
Conduction-band parameters		
m_e^*/m_0	0.0665	0.023
nonparabolicity γ[b] (10^{-15} cm^2)	3.77	31.5
Valence-band parameters		
γ_1	6.85	20.4
γ_2	2.10	8.3
Unstrained energy gaps E_G^0 (eV)	1.5192	0.418
Spin-orbit-split Δ (eV)	0.341	0.381

[a]*International Tables for X-Ray-Crystallography*, edited by J. Ibers and W. C. Hamilton (Kynoch, Birmingham, 1974), Vol. IV.

[b]Calculated from a conduction-band dispersion relation $E(k)=(\hbar^2k^2/2m_e^*)(1-\gamma k^2)$.

$-(\alpha-\Theta_B)]$ is the direction cosine of the diffracted beam.

The "*phase shift parameter,*" i.e., the product of layer thickness and angular deviation from the exact Bragg condition due to the different lattice constants of InAs and GaAs, respectively, is 31.55 nm mrad for 1-ML InAs.[13] The values for the structure factors, elastic stiffness constants, and lattice parameters used for the computer simulation are summarized in Table I. The computer simulation is performed using the dynamical x-ray-scattering theory.[13]

Figure 1 shows the symmetrical (400) and asymmetrical (442) diffraction pattern of the sample under consideration. Note the excellent agreement between the experimental and simulated diffraction profiles. From the simulation we obtain an InAs layer thickness of 3.9±0.15 Å, which corresponds to 1.2±0.05 ML InAs, assuming a lattice strain (x-ray strain) of 14.95% along the ⟨100⟩ direction. The simulation gives evidence for the coherent growth of the InAs monolayer, i.e., the lattice mismatch is accommodated entirely by an elastic tetragonal distortion of the InAs unit cell. This result is confirmed by the x-ray reflection topograph of the structure, where misfit dislocations generated at the highly strained InAs/GaAs interface are not observed.

In addition, the structural properties of the InAs layer are studied by means of HRTEM. In Fig. 2, a high-resolution lattice image of the heterostructure is shown. The projected InAs layer appears as a dark line in the brighter GaAs matrix. The projected thickness of the InAs layer is found to be between 1 and 2 ML, in excel-

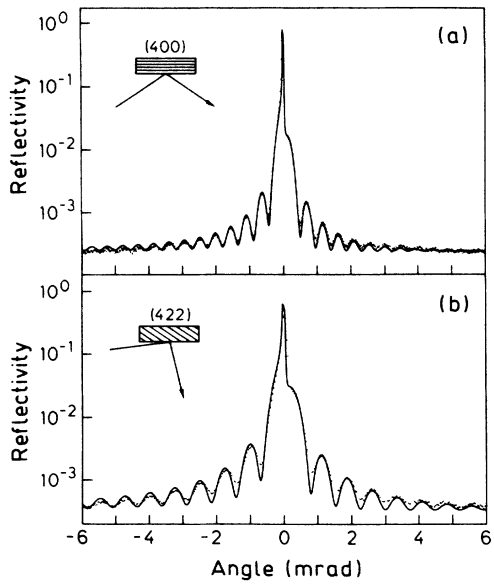

FIG. 1. Experimental (dotted line) and simulated (solid line) x-ray-diffraction patterns in the vicinity of (a) the symmetrical (400) reflection and (b) the asymmetrical (422) reflection, respectively, with $Cu_{K\alpha_1}$ radiation for a heterostructure consisting of 1.2 ML (100) InAs on 1 μm GaAs and capped with 200 nm GaAs.

lent agreement with the HRDXD results. Since the layer thickness exceeds 1 ML, the interface between InAs and GaAs, in principle, cannot be perfectly atomically flat. In fact, the HRTEM image reveals single atomic steps with an average distance of about 10 nm (see Fig. 2). To get reliable quantitative information from these measurements, detailed computer simulations were performed, which will be the subject of a forthcoming publication.[14]

The combination of HRDXD and HRTEM thus allows us to perform an accurate determination of the structural properties, i.e., the lattice strain and the thickness of ultrathin InAs layers embedded in bulklike GaAs. Additionally, by correlating with the growth conditions, these techniques become powerful tools to study the fundamental growth processes in the epitaxy of highly strained systems. In particular, the measured InAs layer thickness of 1.2 ML is found to be significantly smaller than the thickness derived from the measured growth rate of bulk InAs and the beam equivalent pressures before growth. The ratio of the InAs growth rates for 1 ML on GaAs and for bulk material, respectively, is estimated to be 0.64. This value is in accordance with the ratio of the activation energies for the desorption of In from a strained and an unstrained surface, respectively, as determined by Evans *et al.*[8] to about 0.65 for temperatures below 650 °C. Thus, the high lattice strain apparently acts as a kinetic barrier for the incorporation of the cations in the crystal lattice.

If the thickness of a thin highly strained epitaxial layer is derived simply by considering the bulk growth rate, the *actual* thickness of the layer can be much smaller than anticipated. In addition, at higher growth temperatures other processes such as the evaporation and migration of In can be of increasing importance and can further decrease the real amount of cations incorporated in the crystal matrix. Obviously, a lack of knowledge of the precise thickness and—if a migration process takes place—of the composition of strained quantum wells leads to unreliable interpretations of optical data, especially for ultrathin quantum wells. Here, we unambiguously prove the existence of a strained InAs lattice plane with a thickness of 1.2 ML. In addition, we show that no interdiffusion of the strained interfaces takes place, which we mainly attribute to the low growth temperature (420 °C). The excellent homogeneity and the near atomic flatness of the InAs plane is most likely the result of the careful annealing process during the growth interruptions.

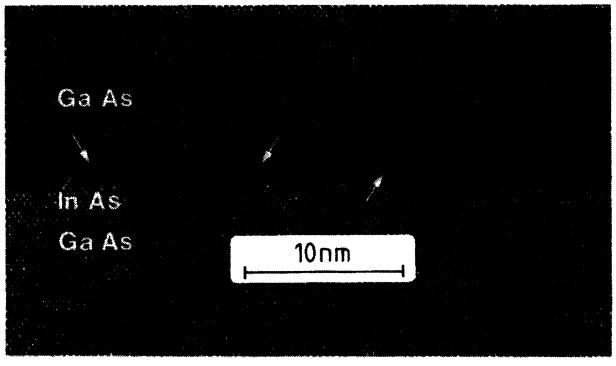

FIG. 2. High-resolution lattice image of the heterostructure under consideration. The (100) InAs lattice plane appears as a dark line in the GaAs matrix. The projected layer thickness fluctuates between 1 and 2 ML. The mean lateral distance between single atomic steps is found to be typically of the order of 8 nm, as indicated by arrows.

B. Optical properties

The PL and PLE spectra recorded at 4.2 K are displayed in Fig. 3. The PL spectrum is dominated by a strong luminescence line at 1.417 eV, which does not appear in a reference sample without the InAs monolayer. The emission lines at 1.516 and 1.49 eV are observed in both samples and can be identified as the free exciton (X) and the donor-acceptor (D^0,C^0) luminescence in GaAs, respectively. The appearance of these two high-energy lines demonstrate the high quality of the structure with the inserted highly strained InAs plane. in particular, the introduction of one highly strained lattice plane apparently does not affect the electronic properties of the GaAs matrix. The PLE spectrum shown in Fig. 3 exhibits two weak transitions at 1.430 and 1.448 eV in addition to the strong resonance at 1.516 eV related to free excitons in GaAs.

In order to identify the transitions found in the PL and PLE spectra, we have calculated the energies of the electron and hole subbands confined in a finite potential well within the envelope-function model, taking into account the influence of strain and conduction-band nonparabolicity. Both these effects have a large impact on the subband energies of small-gap and highly strained systems such as InAs/GaAs. It is worth mentioning that we do not use any adjustable parameter to fit the experimental results. Briefly, we take the experimental valence-band

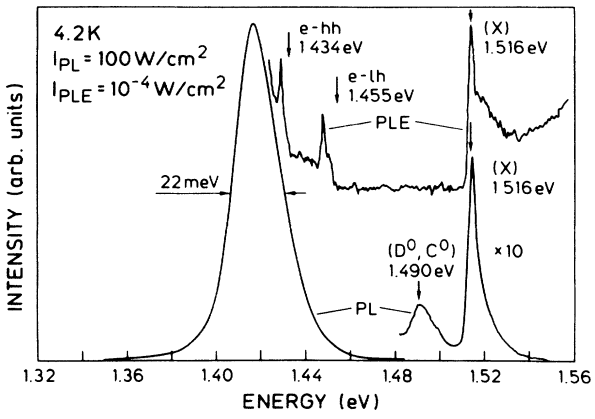

FIG. 3. PL and PLE spectra obtained at 4.2 K from the SQW sample described in the text. The vertical arrows indicate the calculated energy positions for the electron-heavy-hole transition (e-hh) and the electron–light-hole (e-lh) transition, respectively. In addition, the literature values for the luminescence of free excitons (X) and of the donor-carbon transition (D^0,C^0) in bulklike GaAs are also marked by arrows.

offset for the unstrained heterostructure[15] and correct this value for the strain dependence of the band structure of InAs. For an accurate determination of the strain-induced splitting of the v_1 ($|\frac{3}{2},\pm\frac{3}{2}\rangle$) and the v_2 ($|\frac{3}{2},\pm\frac{1}{2}\rangle$) doublet, respectively, it is important to consider the nonlinear terms for the strain correction resulting from the interaction of the two $|J,\pm\frac{1}{2}\rangle$ doublets.[17] Hereafter, the strain-corrected band offsets ΔE_c, ΔE_v^{hh}, and ΔE_v^{lh} (see Fig. 4) are used as fixed input parameters in a multiband Kronig-Penney model for the estimation of the subband energies. For the ground state, the results are insensitive to the nonparabolicity even for a monolayer quantum well. The parameters used for the calculation are given in Table I. The k-space band structure and the real-space band alignment of an InAs/GaAs heterostructure are schematically depicted in Fig. 4. Note that for a **k** vector perpendicular to the layer plane, the band dispersion retains essentially the bulk character. We refer therefore to the upwards-shifted $|\frac{3}{2},\pm\frac{3}{2}\rangle$ doublet as the heavy-hole band and the downward-shifted $|\frac{3}{2},\pm\frac{1}{2}\rangle$ doublet as the light-hole band, respectively. The main impact of the strain is the different valence-band step for the heavy and the light holes. In particular, for the valence-band offset derived as described above, the light holes are still weakly localized in the InAs plane. The results of the calculations for a 3.9-Å InAs quantum well are depicted by the arrows in Fig. 3. Despite the principal limitations of the envelope-function approximation in the limit of ultranarrow wells, we found a reasonable agreement between experiment and calculations. In Table II we summarize the results of the calculations as indicated in Fig. 4. A detailed description of our model will be published elsewhere.[18]

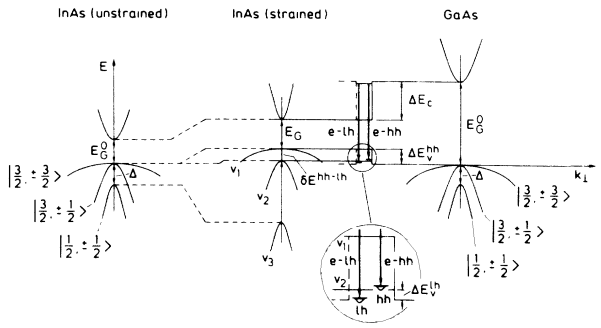

FIG. 4. Scheme of the k-space band structure and the real-space band alignment of an InAs/GaAs heterostructure. The unstrained band structures of InAs and GaAs are sketched in the left and right part of the figure, respectively. The dashed lines show the shift of the InAs band edges under a compressive strain. The strain-modified band structure of InAs is depicted in the center. The solid lines between the InAs and GaAs band edges indicate the conduction- and valence-band offsets. The electron and hole states are represented by horizontal lines in the confining potential step, which is indicated by the dash-dotted lines. In the lower part of the figure the confined heavy-hole and light-hole states are shown in magnification. The optical transitions between these states as discussed in the text are indicated by arrows and are labeled according to Fig. 3. The values for the band gaps, the band offsets, and the strain-induced splitting between the v_1 ($|\frac{3}{2},\pm\frac{3}{2}\rangle$) and the v_2 ($|\frac{3}{2},\pm\frac{1}{2}\rangle$) doublet as estimated in the calculations are listed below: $E_{G\,(\mathrm{InAs})}^0=0.418$ eV, $E_{G\,(\mathrm{GaAs})}^0=1.519$ eV, $E_{G\,(\mathrm{InAs})}=0.531$ eV, $\Delta E_c=0.711$ eV, $\Delta E_v^{hh}=0.277$ eV, $\Delta E_v^{lh}=0.030$ eV, and $\delta E^{hh\text{-}lh}=0.247$ eV.

According to the calculations described above, the strong line at 1.417 eV in the PL spectrum of Fig. 3 is attributed to a transition between the electron and heavy-hole subband confined in a 3.9-Å InAs quantum well. The full width at half maximum (FWHM) of this line is determined to be about 22 meV, which is broader than recently reported values for similar structures grown with advanced epitaxial techniques as atomic-layer epitaxy (ALE),[5] migration-enhanced epitaxy (MEE),[6] and flow-rate modulation epitaxy (FME).[7] All these techniques make use of an alternate supply of the group-III and -V elements in order to improve the cation surface mobility. The enhanced cation migration during the metal-rich cycles is believed to smooth the interfaces as compared to conventional growth techniques like MOVPE and MBE. However, as already stated above, a reliable interpretation of the optical data requires the accurate determination of the structural properties of the strained layer. In particular, a narrow PL linewidth is not in general a direct measure for sharp heterointerfaces. For instance, in Ref. 7 the PL spectrum exhibits a narrow (3.2 meV) and intense line at 1.483 eV, which the authors attribute to the emission from an InAs quantum well with a thickness of 1 ML. In addition, they observe an increase of the PL transition energy with decreasing coverage of the lattice plane with In even for a thickness of the quantum well below 1 ML, i.e., for an incomplete monolayer. Obviously, this finding gives evidence for alloy formation rather than for the growth of pure InAs, partly replaced by GaAs islands. The influence of interface roughness on the PL linewidth is therefore drastically reduced due to the weak confinement of the carriers in the shallow potential step of the ternary $In_xGa_{1-x}As$ layer. Thus, the narrow linewidth as well as the relatively high energy of the quantum-well transition are consistent with the assumption of an alloy formation instead of the growth of a pure binary InAs monolayer. This is again demonstrating the well-known fact that no quantitative information on the structural properties (e.g., the interface roughness) can be obtained by simply considering the luminescence linewidth.[19] In the next section we will therefore discuss in more detail the correlation between structural and optical properties of an InAs monolayer quantum well in the GaAs host material.

TABLE II. Comparison between the experimental and the calculated values for the optical transitions in the investigated heterostructure. The values are expressed in eV and are labeled following the notation of Figs. 3 and 4.

Transition	Theory	Experiment
e-hh (PL)	1.434	1.417
e-hh (PLE)	1.434	1.430
e-ln (PLE)	1.455	1.448

IV. DISCUSSION

According to the model of Singh and Bajaj,[20] the influence of well-width fluctuations on the PL linewidth depends on the step size and the lateral extent of the islands with respect to the exciton radius in the well layer. Taking the average well width of 3.9 Å (1.2 ML) derived in the preceding paragraph, and assuming a total well-width fluctuation of 1 ML and a lateral island extent comparable to the exciton radius, a linewidth of 40 meV is expected, about twice the observed linewidth of 22 meV. Since the lateral island size is the only independent parameter (the value for the island height is established by the HRTEM lattice image), setting the lateral extent of the island to about $R_{ex}/2$ gives the best agreement with the experiment. Note that this value is comparable to the lateral distance of single atomic steps of about 10 nm, which is actually found in the HRTEM lattice image of the InAs monolayer (see Fig. 2). Thus, our simple analysis of the PL linewidth is apparently valid even in the limit of monolayer quantum wells. Further investigations of the correlation between the island size and the optical properties, especially of submonolayer quantum wells, will be published elsewhere.[21]

The pseudosmooth interfaces are known to produce a Gaussian linewidth broadening[22] which we in fact observe. In addition, the different well widths experienced by the excitons result in statistical fluctuations of the fundamental band edge. Hence, the excitonic absorption resonance should be blue shifted (Stokes shift) as compared to the maximum of the luminescence line. In fact, we find a Stokes shift between the first excitonic resonance in PLE at 1.430 eV and the quantum-well luminescence at 1.417 eV of about 13 meV. For the case of ultrathin wells, a well-width fluctuation of 1 ML is expected to have a strong influence on the quantized energy levels of the carriers. Within the envelope-function model, the total band-edge fluctuation corresponds to a maximum Stokes shift of about 55 meV. However, a pseudosmooth interface as indicated by the linewidth analysis would result in a smaller Stokes shift as is actually found. Thus, the luminescence linewidth and the Stokes shift can be explained in terms of a monolayer fluctuation of the well width with a lateral extent of the islands less than the exciton radius, in excellent agreement with the structural investigations by HRTEM and HRDXD.

To the best of our knowledge, the PLE spectrum of Fig. 3 exhibits the first observed excitonic resonances for a single-monolayer quantum well. The high luminescence efficiency of the quantum-well recombination, which allows us to obtain the excitonic resonances even in a single–quantum-well (SQW) sample, can be understood by taking into account the superior optical confinement in the InAs/GaAs heterostructure. In contrast to GaAs/$Al_xGa_{1-x}As$ single quantum wells grown on GaAs, where the luminescence can be self-absorbed in the lower-band-gap GaAs buffer, in InAs/GaAs SQW structures the internal photon loss mechanisms are suppressed by the higher gap buffer.

Another feature of particular interest observed in the PLE spectrum is the peak at 1.448 eV, which we attribute to a light-hole excitonic resonance in accordance with our calculations. In fact, the experimental splitting of the heavy- and light-hole excitonic resonances agrees very well with the theoretical prediction (see Table II). It is important to note that the energy position and the oscillator strength of the light-hole transition are extremely sensitive to the valence-band offset. In contrast to the heavy-hole resonance, the light-hole transition is therefore a reactive probe for the valence-band offset. The striking result of our measurements is that the light holes are still weakly confined in the InAs quantum well, as can be seen by the relatively high oscillator strength comparable to the heavy-hole excitonic resonance. This experimental finding thus confirms the valence-band offset derived from some recent optical investigations of the $In_xGa_{1-x}As$/GaAs system.[3,23] Due to the nonlinear strain dependence of the light-hole band, the results of Refs. 3 and 21 predict a type-I band alignment for *both* the heavy holes and the light holes at $x=1$. However, since the sum of the strain-induced splitting of the light and heavy holes and the confinement energy of the light holes is comparable to the valence-band offset (see Fig. 4), the localization depends critically on the strain state of InAs. Indeed, a slight relaxation causes a smaller valence-band offset and therefore a type-II band alignment for the light hole even at $x>0.6$. As already mentioned, the usual practice to derive the thickness and the composition of a strained layer from bulk growth rates or the beam equivalent pressures of the constituent elements is insufficient to determine important parameters, such as the critical thickness of the strained layer. Thus, by taking into account the weak localization of the light holes in the quantum-well region and the strong strain dependence of the valence-band edges, our results probably provide a plausible explanation for the large discrepancies for the valence-band offset in previously published experiments.

A striking feature of the PL spectrum shown in Fig. 3 is the extremely high luminescence efficiency of the quantum-well recombination with respect to the GaAs band-edge emission. The integrated intensity of the 1.417-eV line is more than 1 order of magnitude higher than that of the GaAs band-edge emission. This result indicates an extremely effective bypass of the radiative-recombination channels in GaAs. Thus in the present case the transfer and capture of photogenerated carriers must be very fast. Assuming an additional flux of photogenerated carriers from the excited GaAs volume to the quantum well and neglecting the QW absorption itself, we can express the ratio of the integrated photoluminescence intensities of the quantum-well transition (L^{QW}) and the GaAs band-edge emission (L^{GaAs}) as

$$\frac{L^{QW}}{L^{GaAs}}=\frac{\tau_r^{GaAs}}{\tau^{QW}} . \tag{2}$$

Here, τ_r^{GaAs} is the effective radiative lifetime in GaAs and τ^{QW} the effective trapping time of the photoexcited carriers into the quantum well, respectively. Since the effective radiative lifetime in high-quality bulk GaAs corresponds to the excitonic lifetime τ_{exc}, we have

$$\tau_r^{\mathrm{GaAs}} = \tau_{\mathrm{exc}}^{\mathrm{GaAs}} \simeq 10^{-9} \text{ s} . \quad (3)$$

Hence, this estimate provides a rough determination of the effective trapping time of the carriers into the InAs monolayer quantum well:

$$\tau^{\mathrm{QW}} \simeq 20 \text{ ps} . \quad (4)$$

This extremely short trapping time gives a plausible explanation for the observed high luminescence efficiency of the radiative transition related to the InAs monolayer quantum well. In terms of a diffusion velocity, we obtain

$$v_{\mathrm{diff}} = 2.5 \times 10^6 \text{ cm/s} , \quad (5)$$

assuming a carrier generation depth of 0.5 μm. This value agrees well with the findings of other authors.[24] However, a detailed investigation of the carrier capture in ultrathin quantum wells is still lacking. Time-resolved measurements providing a deeper insight in the fundamental processes of carrier relaxation, transport, capture, and recombination are underway in this laboratory. A better understanding of these phenomena is highly desirable not only for fundamental aspects but also for device applications in order to improve the emission performance of quantum-well lasers fabricated from this material system.

Finally, it should be mentioned that PL measurements alone are not useful to characterize strain relaxation in highly strained layers. Of course the radiative transition rate depends primarily on the intrinsic recombination properties of the material *and* the type and concentration of electrically active impurities (recombination centers) in the crystal. It is hence reasonable to assume that the generation of misfit dislocations acting as deep traps for the carriers strongly decreases the radiative transition rate, i.e., the luminescence efficiency. However, we want to point out that a decrease of luminescence efficiency *alone* is not a sufficient criterion to consider strain relaxation. For instance, we observe a drastic deterioration of the luminescence characteristics for samples grown under conditions only slightly modified to those described above, i.e., with a higher growth rate and shorter growth interruptions. The important point is that these samples are still of excellent crystalline quality and do *not* exhibit any strain relaxation. The reason for this particular dependence of the luminescence characteristics on growth conditions is not yet fully understood, but it emphasizes the need for further detailed structural and optical investigations of this important strained-layer system.

V. CONCLUSION

In summary, we have performed a detailed structural and optical characterization of highly strained single (100) InAs monolayer quantum wells grown for the first time by conventional molecular-beam epitaxy. The detailed structural investigation by means of HRDXD has proved a superior crystalline quality of the sample. The highly strained InAs monolayer was found to be grown coherently on the GaAs buffer, without any strain relaxation. In agreement with the HRDXD results, in double-crystal x-ray reflection topography no misfit dislocations at the highly strained InAs/GaAs heterointerface were detected. In addition, the HRTEM lattice image of the InAs plane has revealed an excellent homogeneity and atomic flatness of the layer. By correlating with the growth process, this result was attributed to the proper choice of the growth conditions during the deposition of the InAs monolayer. Additionally, it was found that the strain strongly influences the incorporation of cations in the crystal lattice during epitaxial growth. The ratio of the InAs growth rates for 1 ML on (100) GaAs and for bulk material, respectively, was determined to be 0.64. Thus, for a correct interpretation of the optical properties of the samples, a precise determination of the structural parameters is definitely required. With the knowledge of the atomic scale structure of the InAs plane, the observed features in the PL and PLE spectra could be well understood. In particular, the results of our structural investigations support a simple analysis of the PL linewidth and the blue shift (Stokes shift) of the heavy-hole exciton resonance in PLE with respect to the electron–heavy-hole transition in PL. Both the PL linewidth and the Stokes shift were explained with a fluctuation of the well width of 1 ML and a lateral island size of about 10 nm, in excellent agreement with the results of the HRTEM investigation.

The important result of our investigation is that a single-monolayer InAs does indeed yield a pronounced redshift of the quantum-well luminescence with respect to the GaAs band-edge emission. In addition, the observed light-hole exciton resonance in the PLE spectrum has provided direct experimental evidence for a confinement of the light-hole excitons in the InAs plane. Thus, our results support a type-I model for the light-hole confinement as predicted from a simple envelope-function calculation. Finally, the surprisingly high luminescence efficiency was found to be the result of an efficient carrier trapping into the monolayer quantum well with effective trapping times of the order of about 20 ps, indicating the potential of this system for application in optoelectronic devices.

ACKNOWLEDGMENTS

One of us (O.B.) would like to thank A. Fischer for his expert advice on MBE growth. Thanks are due to M. Kelsch for the preparation of the HRTEM samples. This work has been partly supported by the Bundesministerium für Forschung und Technologie (Bonn, Germany) of the Federal Republic of Germany.

[1] E. P. O'Reilly, Semicond. Sci. Technol. **4**, 121 (1989).
[2] H. Munekata, L. L. Chang, S. C. Woronick, and Y. H. Kao, J. Cryst. Growth **81**, 237 (1987).
[3] D. Gershoni, J. M. Vandenberg, S. N. G. Chu, H. Temkin, T. Tanbun-Ek, and R. A. Logan, Phys. Rev. B **40**, 10 017 (1989).
[4] F. Houzay, C. Guille, J. M. Moison, P. Henoc, and F. Barthe, J. Cryst. Growth **81**, 67 (1987).
[5] M. A. Tischler, N. G. Anderson, and S. M. Bedair, Appl. Phys.

Lett. **49**, 1199 (1986).
[6]J. M. Gerard and J. Y. Marzin, Appl. Phys. Lett. **53**, 568 (1988).
[7]M. Sato and Y. Horikoshi, J. Appl. Phys. **66**, 851 (1989).
[8]K. R. Evans, C. E. Stutz, D. K. Lorance, and R. L. Jones, J. Vac. Sci. Technol. B **7**, 259 (1989).
[9]K. J. Monserrat, J. N. Tothill, J. Haigh, R. H. Moss, C. S. Baxter, and W. M. Stobbs, J. Cryst. Growth **93**, 466 (1988).
[10]F. Iikawa, P. Motisuke, J. A. Brum, M. A. Sacilotti, A. P. Roth, and R. A. Masut, J. Cryst. Growth **93**, 336 (1988).
[11]C. Guille, F. Houzay, J. M. Moison, and F. Barthe, Surf. Sci. **189/190**, 1041 (1987).
[12]L. Tapfer and K. Ploog, Phys. Rev. B **40**, 9802 (1989).
[13]L. Tapfer, M. Ospelt, and H. von Känel, J. Appl. Phys. **67**, 1298 (1990).
[14]M. Hohenstein, F. Phillipp, O. Brandt, L. Tapfer, and K. Ploog (unpublished results).
[15]R. S. Bauer and G. Margaritondo, Phys. Today **40**(1), 27 (1987), and references therein.
[16]*Landolt-Börnstein, Numerical Data and Functional Relationships in Science and Technology, New Series III/17a,* edited by O. Madelung, M. Schulz, and H. Weiss (Springer, Heidelberg, 1982).
[17]F. H. Pollak and M. Cardona, Phys. Rev. **172**, 816 (1968).
[18]O. Brandt, R. Cingolani, L. Tapfer, and K. Ploog (unpublished results).
[19]R. C. Miller and R. Bhat, J. Appl. Phys. **64**, 3647 (1988).
[20]J. Singh and K. K. Bajaj, J. Appl. Phys. **57**, 5433 (1985).
[21]R. Cingolani, O. Brandt, L. Tapfer, G. Scamarcio, and K. Ploog (unpublished results).
[22]E. F. Schubert and W. T. Tsang, Phys. Rev. B **34**, 2991 (1986).
[23]S. H. Pan, H. Shen, Z. Hang, F. H. Pollak, W. Zhuang, Q. Xu, A. P. Roth, R. A. Masut, C. Lacelle, and D. Morris, Phys. Rev. B **38**, 3375 (1988).
[24]E. O. Göbel, H. Jung, J. Kuhl, and K. Ploog, Phys. Rev. Lett. **51**, 1588 (1983), and references therein.

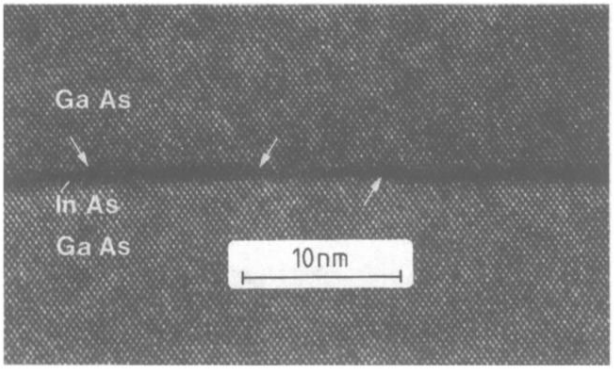

FIG. 2. High-resolution lattice image of the heterostructure under consideration. The (100) InAs lattice plane appears as a dark line in the GaAs matrix. The projected layer thickness fluctuates between 1 and 2 ML. The mean lateral distance between single atomic steps is found to be typically of the order of 8 nm, as indicated by arrows.